

Palindrome Remote Sensing GmbH

---

# **RAdar Simulation of wind Turbines (RAST)**

## **Radar Simulation Model Description**

---



*Authors:*  
Marc Schneebeili  
Andreas Leuenberger

*Palindrome Remote Sensing GmbH, Landquart*

Version 0.7

November 17, 2022



# Document Administration

## Version Control

Version	Edited by	Date	Action
0.1	A. Leuenberger	May 18, 2021	Creation
0.2	A. Leuenberger	June 23, 2021	Chapter Simulations added
0.3	A. Leuenberger	June 28, 2021	Chapter Measurements added
0.4	M. Schneebeli	September 28, 2021	Chapter Introduction added
0.5	M. Schneebeli	October 29, 2021	Revision and submission to BFE
0.6	A. Leuenberger	February 23, 2022	Added straight wire blade model and multiple windmills
0.7	A. Leuenberger	November 17, 2022	Added measurements of multiple windmill simulations
0.8	M. Schneebeli	November 18, 2022	Added windpark measurement description. Proof reading and submission.



# Contents

<b>1</b>	<b>Introduction</b>	<b>1</b>
<b>2</b>	<b>The Windmill Simulator</b>	<b>3</b>
2.1	Overview . . . . .	3
2.2	Basic Theory . . . . .	3
2.2.1	Radar Equation . . . . .	3
2.2.2	Frequency Spectrum . . . . .	4
2.3	Windmill Simulation Overview . . . . .	4
2.4	Replay Block . . . . .	5
2.5	Modulation Stream . . . . .	5
2.5.1	Point Scatterers . . . . .	5
2.5.2	Straight Wire Scatterer . . . . .	7
2.6	Wind Farms . . . . .	7
<b>3</b>	<b>Simulations</b>	<b>9</b>
3.1	Simulation Setup . . . . .	9
3.2	Most Simple Simulation . . . . .	9
3.3	Blade Flash . . . . .	10
3.4	Blade Simulated by Four Spheres . . . . .	11
3.5	Three Blades . . . . .	11
3.6	Combination of Point Scatterers . . . . .	12
3.7	Straight Wire Scatterer . . . . .	13
3.8	Wind Farms . . . . .	13
3.8.1	Two Windmills . . . . .	13
3.8.2	Three Windmills . . . . .	13
<b>4</b>	<b>Measurements</b>	<b>17</b>
4.1	Overview and Setup . . . . .	17
4.1.1	Windpark measurements . . . . .	18
4.2	Windmill Measurements . . . . .	21
4.3	Measurements of Simulated Windmills and Wind Parks . . . . .	21
4.3.1	Simple Windmill Simulation . . . . .	21
4.3.2	Windpark simulation set-up . . . . .	22
4.3.3	Wind Park with Two Windmills . . . . .	22
4.3.4	Wind Park with Four Windmills . . . . .	23
4.4	Validation . . . . .	25
<b>5</b>	<b>Outlook</b>	<b>27</b>
	<b>Acronyms and Glossary</b>	<b>29</b>



# Chapter 1

## Introduction

Wind turbines have a perturbative influence on air traffic control radars (radars operated by Skyguide and by the air force) as well as on meteorological radars that are used for precipitation measurements (radars operated by the Federal Office for Meteorology MeteoSwiss). Wind power projects are declined if it is suspected that a planned turbine might reduce the data quality of the aforementioned institutions. Such conflicts inhibit a production of 14 GWh of wind energy per year. In the context of this project, a radar target simulator is being developed that receives radar signals and re-transmits them with a specific modulation and time delay, such that the signature of one or several wind turbines appear on the screen of the radar under test. The radar compatibility of the wind turbine project can therefore be assessed and project alterations can be tested in advance with the goal to increase the number of wind farms without hampering the data quality of the radar operators.

In the document at hand, it is described how the radar reflectivity of a wind turbine can be simulated and how such a simulation can be replayed with a radar target simulator (RTS), such that a virtual wind turbine can be generated in the field of view of a radar system. To do so, a simplified physical model is of the back-scattering properties of a wind turbine is being developed in a first step.

This physical model calculates a radar signature (i.e., backscatter intensity — Doppler pattern) as function of time and depending on geometrical and physical properties of the wind turbine. This radar signature is digitized in a form that it can be used to modulate incoming radar pulses. This process is described in Sections 2.3, 2.4 and 2.5.

Radar signatures of wind turbine were measured with a C-band radar. These field measurements are documented in Section 4. In this section, also a first RTS simulation of a wind turbine as seen with the C-band radar is being documented.



# Chapter 2

## The Windmill Simulator

### 2.1 Overview

A windmill seen from a radar perspective can be characterized as a scattering object at a more or less constant distance to the radar but with a varying radar cross section (RCS).

In a first step, the windmill is simplified by assuming that the total back scattering occurs at the same distance to the radar. The RCS is modulated to generate the typical radar characteristics of a windmill.

In a second step, the windmill model is extended to a larger extent in distance. Therefore, the windmill is modeled with a discrete number of single scattering objects at different distances to the radar.

### 2.2 Basic Theory

#### 2.2.1 Radar Equation

We consider a scattering object at a fixed distance  $R$  to a radar. The received power  $p_r$  of a scattering object can be described by the radar equation as

$$p_r = \frac{p_t G^2 \lambda^2}{(4\pi)^3 R^4} \sigma_b, \quad (2.1)$$

where  $p_r$  is the received power,  $p_t$  the transmit power of the radar,  $G$  the antenna gain,  $\lambda$  the wave length,  $\sigma_b$  the radar cross section (RCS) of the scattering object and  $R$  denotes the distance from the radar to the object.

Since a pulsed radar with pulse width  $\tau$  and a pulse repetition interval (PRI) of  $T$  is considered, the received power of a scattering object as a function of time is only valid when the reflected pulse power reaches the receiver:

$$p_r(t) = \Pi(t) \frac{p_t G^2 \lambda^2}{(4\pi)^3 R^4} \sigma_b(t) \quad (2.2)$$

with  $\Pi(t)$  as

$$\Pi(t) = \begin{cases} 0, & \text{if } (t - t_d - lT) < 0 \\ 1, & \text{if } (t - t_d - lT \geq 0) \ \& \ (t - t_d - lT < \tau) \\ 0, & \text{if } (t - t_d - lT) \geq \tau \end{cases} \quad (2.3)$$

$t_d = 2R/c$  is the time of the pulse propagation from the radar to the scattering object and back ( $c$  is the speed of light).  $l$  denotes the  $l^{\text{th}}$  pulse of the radar. It is assumed that the RCS  $\sigma_b(t)$  is not constant and varies in time.

The receive signal  $r(t)$  describes the complex amplitude of the signal received by the radar. The relation between the receive signal  $r(t)$  and the received power  $p_r(t)$  is given by

$$p_r(t) = |r(t)|^2. \quad (2.4)$$

The receive signal  $r(t)$  can be written as

$$r(t) = K \Pi(t) m(t) \quad (2.5)$$

where the constant  $K$  is given by

$$K = \sqrt{\frac{pt G^2 \lambda^2}{(4\pi)^3 R^4}} \quad (2.6)$$

and the term  $m(t)$  represents the modulated RCS.

The complex modulation function  $m(t)$  can be separated into the real function  $m_A(t)$  that modulates the amplitude of the RCS and the function  $\varphi(t)$  that modulates the phase. The following equation shows the relation between  $m(t)$ ,  $m_A(t)$  and  $\varphi(t)$ .

$$m(t) = m_A(t) e^{i\varphi(t)} \quad (2.7)$$

It needs to be noted that variations of the amplitude  $m_A(t)$  are slow and hence assumed to be constant during a coherent processing interval (CPI). It is assumed that

$$\frac{dm_A(t)}{dt} \approx 0, \quad \text{during a CPI.} \quad (2.8)$$

### 2.2.2 Frequency Spectrum

The frequency shift  $f_d(t)$  of the scattering object detected by the radar depends on the change of the phase  $\varphi(t)$  of the received signal  $r(t)$ .

$$f_d(t) = \frac{1}{2\pi} \frac{d\varphi(t)}{dt} \quad (2.9)$$

If the scattering object is moving, the frequency shift  $f_d(t)$  is determined by the Doppler effect

$$f_d(t) = -\frac{2v_r(t)}{\lambda}, \quad (2.10)$$

where  $\lambda$  is the wavelength and  $v_r(t)$  the radial velocity of the scattering object.

The radar signal processor is calculating the frequency spectrum of all range bins during the CPI. The frequency spectrum at range  $R_k$  is using the samples of the received signal with a delay of  $t_{d,k} = 2R_k/c$  after each transmit pulse. The pulse repetition interval (PRI) is given by  $T$  while a CPI consists of  $N$  pulses. The discrete samples at range bin  $k$  during a CPI are given by

$$r_k[l] = r(lT + t_{d,k}), \quad \text{for } (l \in \mathbb{N}_0) \ \& \ (0 \leq l < N). \quad (2.11)$$

The frequency spectrum at range bin  $k$ ,  $S_k(f)$ , is calculated with the discrete fourier transform (DFT) of the discrete receive samples at range bin  $k$  during all pulses  $l$  of a CPI:

$$S_k(f) = \mathcal{F} \{r_k[l]\} \quad (2.12)$$

It is assumed that the variations of the modulation function  $m(t)$  are slow and do not change during the pulse time  $T$ . If the range bin  $k$  is considered as the reflection where the  $\Pi(t)$  function assumes non-zero values, then the receive function  $r(t)$  is sampling the modulation function  $m(t)$  with each pulse or with the PRF.

## 2.3 Windmill Simulation Overview

To generate the characteristics of a windmill seen from a radar, the radar pulses must be modulated by an appropriate modulation function  $m(t)$ . The windmill simulator can be divided into two parts, i.e., the replay block that modulates the radar pulses with a predefined modulation function  $m(t)$  and a software block that generated the samples of the modulation function according to the windmill specification.

In Section 2.4 the functionality of the pulse modulation is described whereas Section 2.5 describes the generation of modulation samples for  $m(t)$ .

## 2.4 Replay Block

The modulation of the radar pulses is performed within the Palindrome radar target simulator (RTS). A picture of the RTS is shown in Figure 4.4.

The pulses from the radar are received by an antenna of the RTS. Received signals are down-converted and digitized. In the FPGA of the RTS the complex samples are being processed. After the digital processing the samples are converted back to an analog signal, up-converted to the radar frequency and transmitted over an antenna towards the radar.

An overview of the signal processing for a windmill simulation is given in Figure 2.1. The down-converted and digitized complex samples are multiplied by the modulation stream. Samples are delayed before they are re-transmitted to the radar. The modulation stream is loaded into the RAM that is connected to the FPGA where it is periodically replayed.

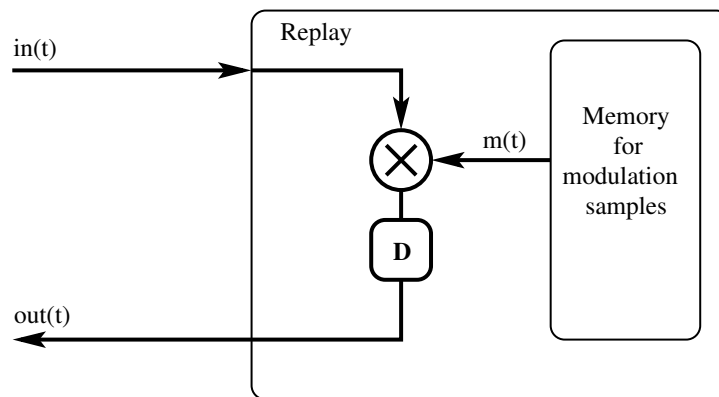


Figure 2.1: Overview of the replay functionality. The incoming samples ( $in(t)$ ) are multiplied with the modulation stream ( $m(t)$ ) and delayed ( $D$ ) before their re-transmission. The samples of the modulation stream are stored in a memory block from where they are periodically replayed.

The windmill characteristics are currently generated with a fixed time delay. The model can however be extended such that multiple modulation chains with different delays become possible.

## 2.5 Modulation Stream

The modulation stream ( $m(t)$ ) is generated by a simple windmill model. The blades are simulated by a combination of a discrete number of point scatterers at different radii (see Section 2.5.1) and straight wire scatterers (see Section 2.5.2).

### 2.5.1 Point Scatterers

Table 2.1 provides an overview of the parameters that are needed to generate the samples for the modulation stream  $m(t)$ .

The duration of the modulation stream  $T_{sim}$  is calculated by Equation 2.13. This sample sequence is repeated in the replay block.

$$T_{sim} = \frac{60}{rpm \times num\_blades} \quad (2.13)$$

The number of simulation samples  $N_{sim}$  is calculated by

$$N_{sim} = T_{sim} \times sample\_rate \quad (2.14)$$

Parameter	Description
sample_rate	Sampling rate (in MHz) at which the modulation stream is generated. This value must correspond to the sampling rate of the RTS.
radar_frequency	Frequency of the radar in MHz.
output_file	Name of the output file containing the samples of the modulation stream. This file is loaded into the data storage of the RTS and periodically replayed by the replay block.
range	Distance from the radar to the simulated windmill in km. The parameter effects the magnitude of the modulation samples. Currently a different scaling is done in the RTS while the file is loaded.
num_blades	Number of blades of the simulated windmill.
rpm	Rotational speed of the windmill in RPM.
rotor_angle	Angle of the rotor plane of the windmill to the radar — windmill direction (in degree).
start_angle	Start angle of first blade in degrees.
num_rcs	Number of point scatterers that are used to simulated a windmill blade.
radius	The radii of the point scatterers in meters. The number of values in this vector must be equal to <i>num_rcs</i> .
rsc	The RCS of the point scatterers in square-meters. The number of values in this vector must be equal to <i>num_rcs</i> .
phase_start	The starting phase in degree of the point scatterers. The number of values in this vector must be equal to <i>num_rcs</i> .
rsc_weighting	A weighting function of each point scatterer during a full rotor revolution. This function is used to generate blade flashes.

Table 2.1: Radar simulation parameters.

The modulation function  $m(t)$  is the superposition of the modulation functions of all point scatterers

$$m(t) = \sum_{b=1}^{\text{num\_blades}} \sum_{k=1}^{\text{num\_rcs}} m_k(t, \beta_b(t)) \quad (2.15)$$

where the function  $m_k(t, \beta_b(t))$  is the modulation function of a point scatterer and the angle  $\beta_b(t)$  is the rotational angle of blade  $b$  at time  $t$ .

The rotational angle  $\beta_b(t)$  (in radians) of blade  $b$  is given by

$$\beta_b(t) = \left[ \frac{60 \cdot 2\pi \cdot t}{\text{rpm}} + b \frac{2\pi}{\text{num\_blades}} \right] \bmod 2\pi \quad (2.16)$$

The distance  $\Delta R_k$  is the range offset of the point scatterer  $k$  to the distance from the radar to the simulated windmill. It is calculated by

$$\Delta R_k = -R_k \cos(\text{rotor\_angle}) \sin(\beta_b(t)) \quad (2.17)$$

The phase change  $\varphi$  of the incoming radar pulse to the reflected radar pulse of the simulated point scatterer is given by

$$\varphi = \left[ \text{phase\_start}_k + \frac{4\pi \Delta R_k}{\lambda} \right] \bmod 2\pi \quad (2.18)$$

where  $\lambda$  is the wavelength.

Finally, the modulation function of the point scatterer  $m_k(t)$  is given by

$$m_k(t, \beta_b(t)) = \sqrt{\text{rsc}_k} w_k(\beta_b(t)) \exp^{i\varphi} \quad (2.19)$$

where  $w_k(\beta_b(t))$  is the weighting function of the point scatterer  $k$ .

## 2.5.2 Straight Wire Scatterer

Since blades are objects with a very large aspect ratio, they can be modeled as one-dimensional objects with constant length  $L$  (see ?, ? and ?). Their radar reflectivity per unit length is given by the function  $\alpha(r)$ , where  $r$  describes the distance from the rotation center.

The return signal from a blade ( $s_{blade}(t)$ ) can be expressed by

$$s_{blade}(t) = e^{i\varphi_0} \int_0^L \alpha(r) e^{-2i \vec{k}_0 \vec{e}_b(t) r} dr \quad (2.20)$$

where  $\varphi_0$  denotes a initial phase offset,  $\vec{k}_0$  is the radar wave vector that defined the direction of the incident wave from the radar and  $\vec{e}_b(t)$  is the unit vector in direction of the blade.

The radar wave vector  $\vec{k}_0$  is given by

$$\vec{k}_0 = \begin{pmatrix} \frac{2\pi}{\lambda} \\ 0 \\ 0 \end{pmatrix} \quad (2.21)$$

and the  $\vec{e}_b$  is given by

$$\vec{e}_b(t) = \begin{pmatrix} -\sin(\beta_b(t)) \\ \cos(\beta_b(t)) \\ 0 \end{pmatrix} \quad (2.22)$$

In a first step, we assume that the specific radar reflectivity  $\alpha(r)$  is constant. Then Equation 2.20 solves to

$$s_{blade}(t) = \alpha L e^{i(\varphi_0 - \vec{k}_0 \vec{e}_b(t) L)} \text{sinc}(\vec{k}_0 \vec{e}_b(t) L) \quad (2.23)$$

Note, that the  $\text{sinc}(x)$  function is defined as  $\sin(x)/x$ .

A straight wire blade is configured by the parameters defined in Table 2.2.

Parameter	Description
wire_enable	True to enable the straight wire blade model.
wire_radius_min	Start radius of straight wire blade in meters.
wire_radius_max	End radius of straight wire blade in meters.
wire_reflectivity	Reflectivity per unit length ( $\alpha$ ) in $m^2/m$ .
wire_phase_offset	Phase offset ( $\varphi_0$ ) in degrees.
wire_view_angle	Incident angle of the radar radiation in degrees (usually $0^\circ$ ).

Table 2.2: Radar simulation parameters for a straight wire.

## 2.6 Wind Farms

The radar signature of a wind farm is described by the sum of the radar signatures of several windmills. Thus, the received signature by the radar (Equation 2.5) extends to

$$r(t) = \sum_{l=1}^N K_l \Pi_l(t) m_l(t) \quad (2.24)$$

for  $N$  windmills. The constant  $K$  (defined by Equation 2.6) changes to  $K_l$  where the distance from the windmill to the radar  $R$  becomes  $R_l$ . In the definition of  $\Pi_l(t)$  (see Equation 2.3) the time constant  $t_d$  changes to  $t_{d,l} = 2 R_l/c$ .

The extended replay block is shown by Figure 2.2. The incoming signal  $in(t)$  is delayed individually for each windmill. The common delay  $D$  corresponds to the nearest windmill with  $D = 2 R_1/c$  and the additional delays  $D_l$  are calculated from the previous delay such that  $D_l = D_{l-1} + 2 (R_l - R_{l-1})/c$ .

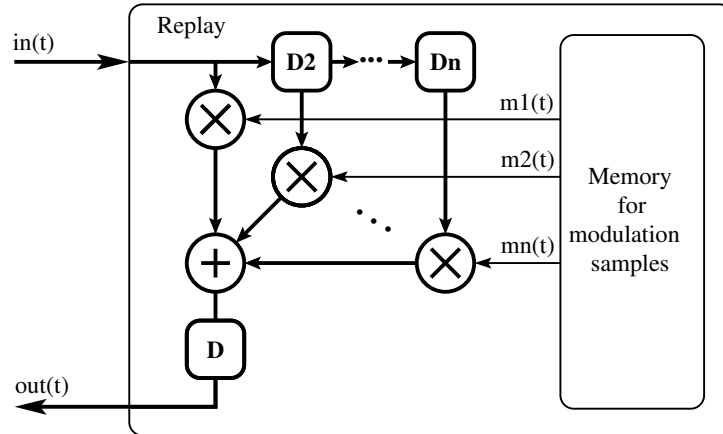


Figure 2.2: Structure of the replay block for a wind farm. Each multiplier modulates the input stream ( $in(t)$ ) with the radar signature of a different windmill.

It is also possible that more than one windmill are located at the same distance. In this case the overall modulation signal  $m(t)$  is the sum of the modulation signals  $m_l(t)$  of all windmills at the same distance.

$$m(t) = \sum_{k=1}^N m_k(t) \quad (2.25)$$

where  $m_l(t)$  is the modulation signal of the  $l^{th}$  windmill given by Equation 2.15.

# Chapter 3

## Simulations

### 3.1 Simulation Setup

Simulations are performed according to the model described in the previous chapter. Simulations with a strongly simplified model are done at the beginning before the model complexity is increased. In Table 3.1 the simulation parameters of the simulated radar and the simulated windmill are listed. For the windmill only the parameters that remain constant during all the simulations are being listed.

Parameter	Value
Frequency	5.35 GHz
Transmit peak power	100 kW
Antenna gain	20 dBi
PRF	20 kHz
Pulse width	2 $\mu$ s
Pulse compression	No
CPI	100 ms
Distance radar to windmill	4 km

Table 3.1: Radar simulation parameters

### 3.2 Most Simple Simulation

The most simple simulation is a windmill with a single blade. The blade is simulated by a sphere with a constant RCS that rotates with a constant rotational speed at a given radius. Figure 3.1 shows the result of this simulation.

The CPI of the simulated radar is 100 ms (i.e., the same CPI that is used for the measurements with the real radar). This relatively long time period leads to the “sampled” micro-Doppler curve. The RCS remains constant during the simulation. Since the Doppler frequency change during a CPI varies, the reflected energy is spread over different frequency ranges.

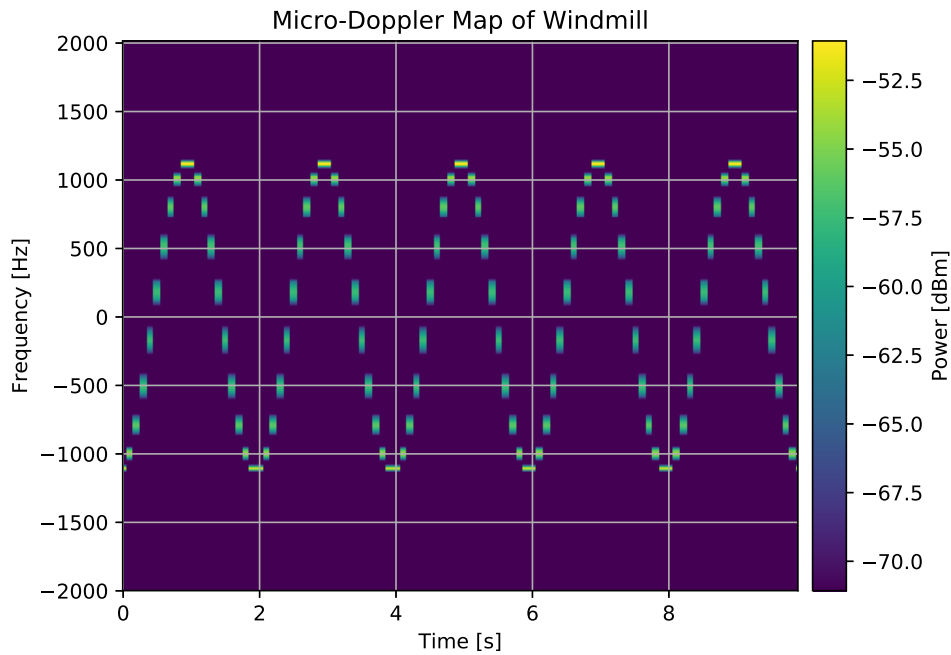


Figure 3.1: Simulation with one blade, 1 scatterer at radius 10 m and a rotational speed of 30 RPM.

### 3.3 Blade Flash

Figure 3.2 shows a simulation of a windmill with one blade, simulated by a sphere at radius 40 m that rotates with 12 RPM. In contrast to the previous simulation, the RCS is not constant during a revolution. A so called *blade flash* during the 3<sup>rd</sup> second is simulated.

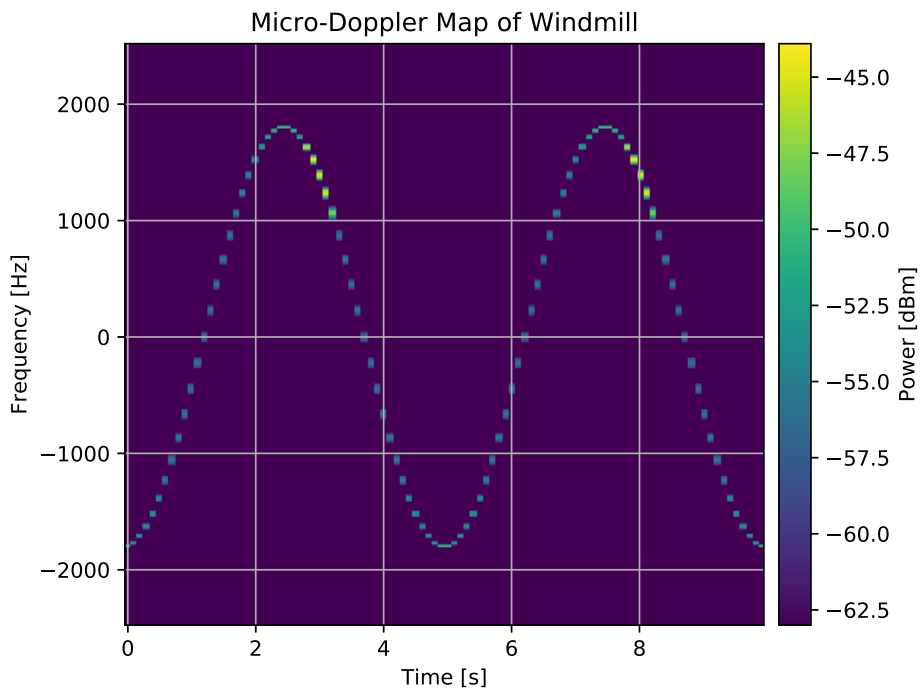


Figure 3.2: Simulation with 1 blade, 12 RPM, blade radius 40 m, blade flash at about 3 and 8 s.

### 3.4 Blade Simulated by Four Spheres

Furthermore, the blade is simulated by 4 spheres with constant RCS. The radii of the spheres are 40, 30, 20 and 10 m. The simulation result is shown in Figure 3.3.

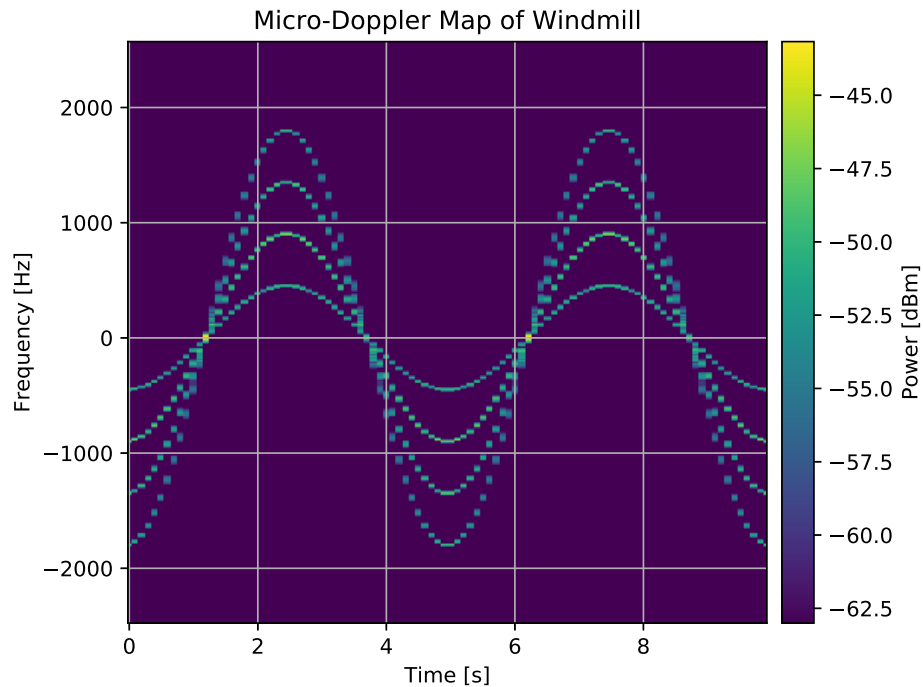


Figure 3.3: Simulation with 1 blade, 12 RPM, blade simulated by 4 spheres with 40, 30, 20 and 10 m radius.

### 3.5 Three Blades

Figure 3.4 shows the micro-Doppler simulation of a windmill with three blades. All blades are simulated by a constant scatterer at a fixed radius.

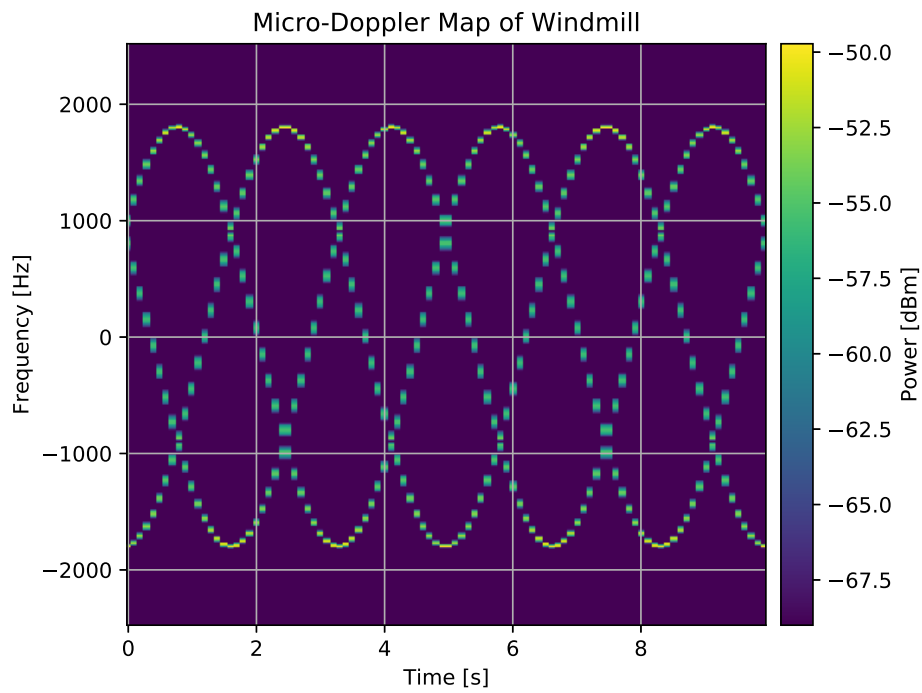


Figure 3.4: Simulation with 3 blades, 12 RPM, blade radius 40 m.

### 3.6 Combination of Point Scatterers

In Figure 3.5 the previously described features are combined: Three blades are simulated with 4 constant scatterers at different radii as well as a blade flash.

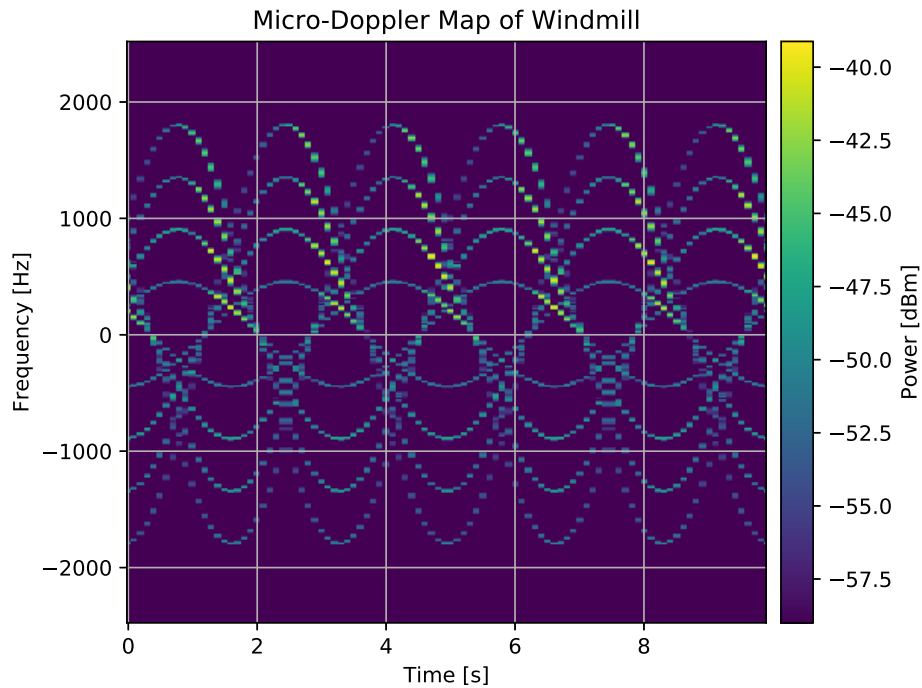


Figure 3.5: Simulation with a combination of all features: 3 blades, blades simulated by 4 spheres at 40, 30, 20 and 10 m radius, blade flash.

### 3.7 Straight Wire Scatterer

Figure 3.6 shows the simulation result of a rotating straight wire blade during two rotations. The blade flashes can be clearly seen when the blade is pointing vertically up- and downward. However the reflections of the blade between two blade flashes can be improved, since almost no echos are visible in the frequency range from zero to the maximal Doppler frequency.

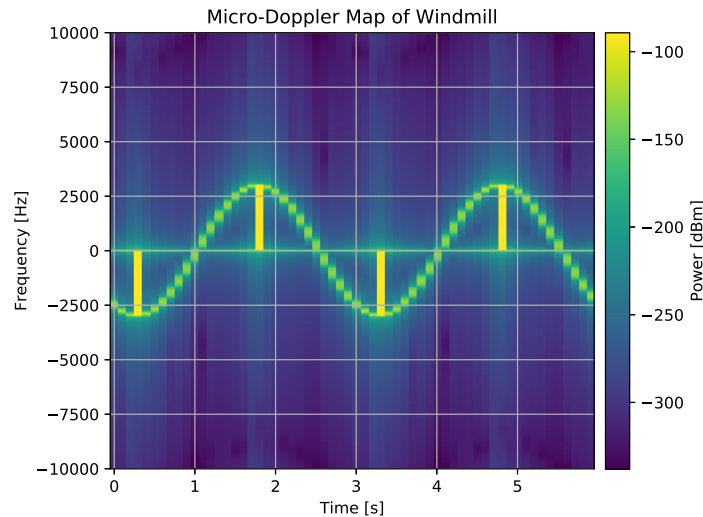


Figure 3.6: Simulation of rotating straight wire blade. The strong yellow reflections are the blade flashes where the blade is perpendicular to the incident radar radiation.

## 3.8 Wind Farms

### 3.8.1 Two Windmills

The most simple wind farm consists of two windmill located at the same distance to the radar. The micro-Doppler signal of such a configuration is shown by Figure 3.7. The rotation speed of the windmills are different, it is 20 RPM for the first and 30 RPM for the second windmill. Because of simplicity reasons, both windmills has only one blade and each blade is simulated by a point scatterer.

In Figure 3.8 two windmills with three blades each are simulated. Each blade is modeled by a set of point scatterers. The reflectivity of the windmill with the smaller Doppler speed is larger.

### 3.8.2 Three Windmills

The micro-Doppler signature of three windmills becomes more unclear. An example is shown in Figure 3.9 where three windmills with different rotation speeds, rotator radii and reflections are simulated. Each windmill has three blades. It can be seen that the signatures of each windmill blur into the others.

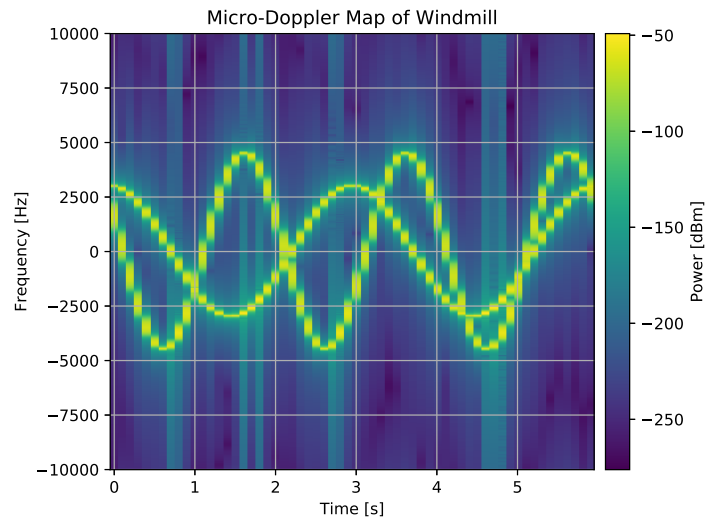


Figure 3.7: Simulation of two windmills with one blade. The rotation speed is 20 RPM for the first and 30 RPM for the second windmill. The blades of both windmills are simulated by a point scatterer with fixed RCS.

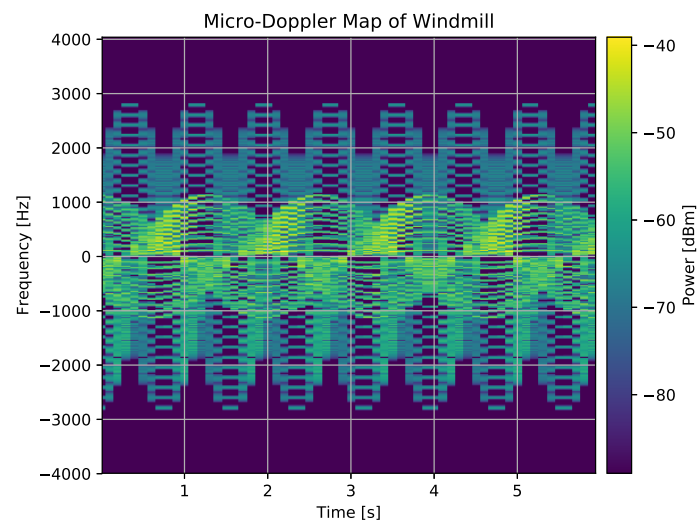


Figure 3.8: Simulation of two windmills with three blades each.

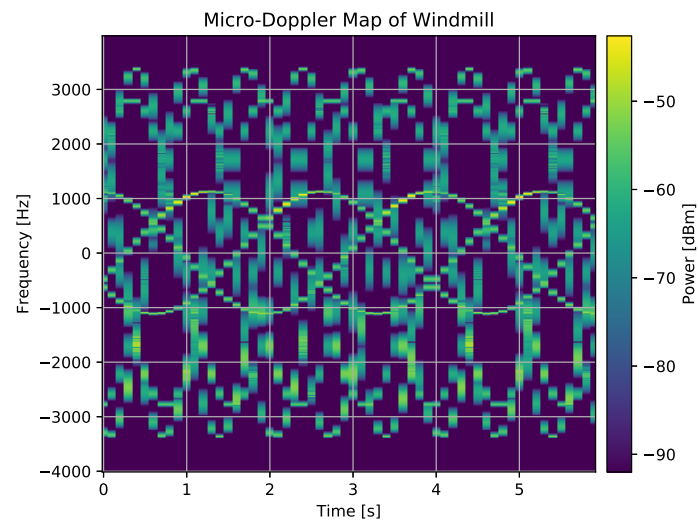


Figure 3.9: Simulation of three windmills with three blades each.



## Chapter 4

# Measurements

### 4.1 Overview and Setup

The first tests with the RTS to simulate a windmill are done near the windmill Calandawind in Haldenstein (near Chur). An overview of the measurement site is given in Figure 4.1. The radar was set up at two locations to measure the micro-Doppler characteristics of the windmill (location *Radar 1*) and the simulated windmill characteristics by the RTS (location *Radar 2*).

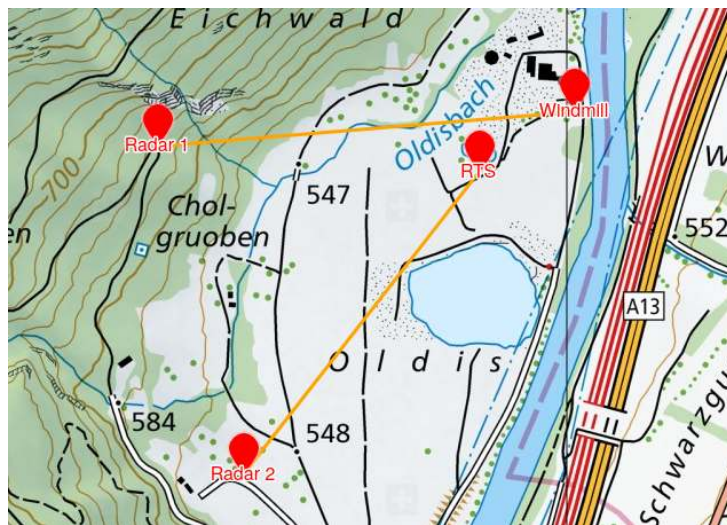


Figure 4.1: Overview of the measurement site in Haldenstein (near Chur). The radar was set up at two locations. From the first radar location (*Radar 1*) the Calandawind windmill (distance 730 m) was measured while from the second location (*Radar 2*) a windmill simulated by the RTS (distance 670 m) was measured.

A picture of the Calandawind windmill is given in Figure 4.2. It was taken at the radar location (*Radar 1*) while the distance from the radar to the windmill is 730 m.

A bi-static C-band radar (Schneebeil et al., 2020) was used to measure the simulated micro-Doppler characteristics (see Figure 4.3). The transmitter and the receiver of the radar were set up next to each other such that the radar was operating in a quasi mono-static mode. The parameters of the radar are listed in Table 4.1.

An image of the RTS is shown by Figure 4.4. The distance from the RTS to the radar was about 670 m. The radar pulses of the radar are delayed such that the simulated windmill occurred at a range of 2 km to the radar.



Figure 4.2: The Calandawind windmill seen from the radar location (*Radar 1*).

Parameter	Value
Frequency	5.35 GHz
Transmit peak power	100 W
PRF	20 kHz
Pulse width	10 $\mu$ s
Pulse compression	Linear chirp up
Pulse bandwidth	20 MHz
CPI	100 ms

Table 4.1: The parameters of the radar.

### 4.1.1 Windpark measurements

A windpark measurement experiment was attempted in La Chaux-de-Fonds with the goal to measure three turbines of the Mont-Soleil windpark. For logistic reasons, the X-band radar of Swiss federal institute of technology in Lausanne (EPFL) was used. The set-up was complemented with an X-band target simulator with the goal to replay the sampled waveform during the same experiment.

Wind park measurements performed in La Chaux-de-Fonds were found to be inconclusive due to Doppler and range resolution limitations. The resulting Doppler spectrograms exhibited a low time resolution that makes it difficult to use them for model development and data can be used for quantitative evaluation only. It was therefore decided to develop a windpark Doppler signature model based on the measurement of a single turbine.



Figure 4.3: Bi-static C-band radar used for the measurements. The transmitter is on the right and the receiver on the left.



Figure 4.4: Image of the radar target simulator (RTS). The radar pulses are received by the round antenna on the right. The modulated and delayed pulses are sent back towards the radar by the antenna on the left.

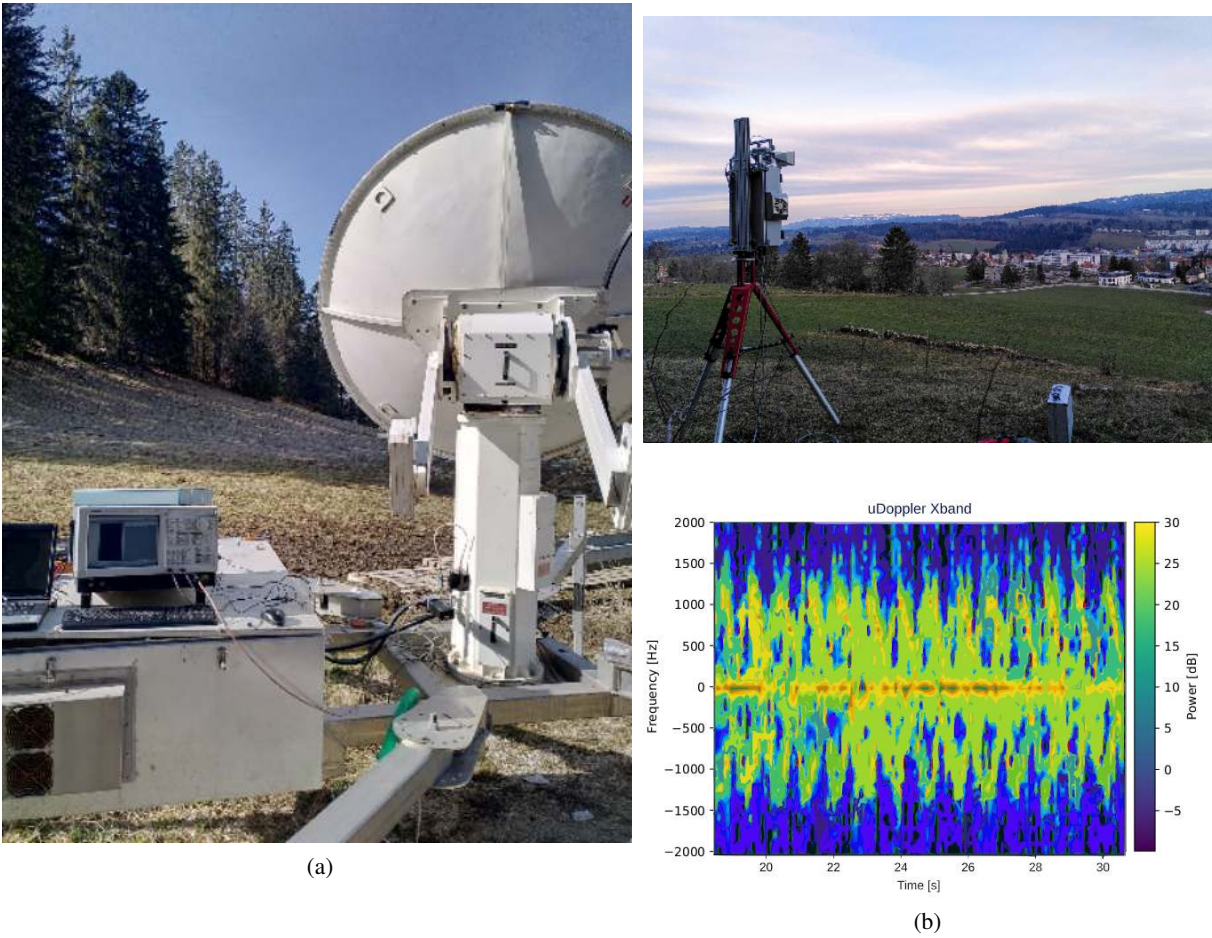


Figure 4.5: (a) EPFL X-band radar used for wind park measurements. (b) Top: RTS overlooking La Chaux-de-Fonds. Bottom: X-band Doppler-RCS measurement of the windpark. Two turbines were located in the radar's field of view.

## 4.2 Windmill Measurements

From the radar location (*Radar 1*) the micro-Doppler characteristics of the windmill were measured. An example of these measurements are depicted in Figure 4.6. The period of a full revolution of the rotor was approximately 7.8 s (corresponding to approximately 7.7 RPM). The strong signal at the zero Doppler frequency is caused by the windmill's mast. The signals that exhibit Doppler frequencies greater than zero stem from blades that move towards the radar. Since the rotation direction during the measurements was counter-clockwise (from the radar point of view), the micro-Doppler signal above zero originated from blades above the rotation center while the signal below the zero Doppler line stem from blades below the rotation center. In the part with negative Doppler frequencies a shaded area can be recognized. This feature was caused when the windmill's mast shielded the blade. Strong echos can be observed when the blades are almost vertical.

The maximum Doppler frequency is about 1400 Hz, corresponding to the Doppler frequency shift caused by the blades with a radius of 50 m rotating at 7.7 RPM and measured at 5.35 GHz.

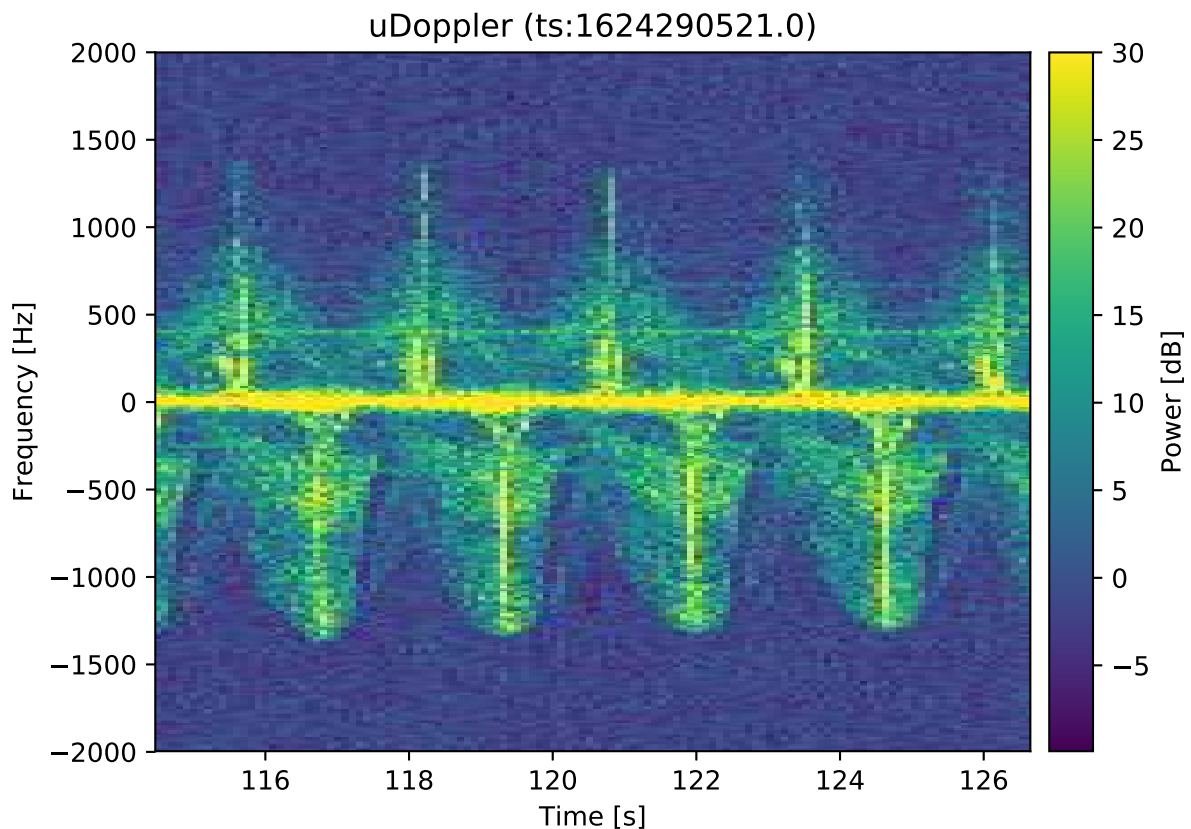


Figure 4.6: Measurements of the Calandawind windmill. Duration of a full rotation is about 7.8 s.

## 4.3 Measurements of Simulated Windmills and Wind Parks

### 4.3.1 Simple Windmill Simulation

The RTS was modulating the radar pulses according the scenario described in Section 3.2. This is the most simple scenario that simulates a rotating sphere. The measured micro-Doppler measurement is shown in Figure 4.7. The measurement corresponds very well to the simulation shown in Figure 3.1.

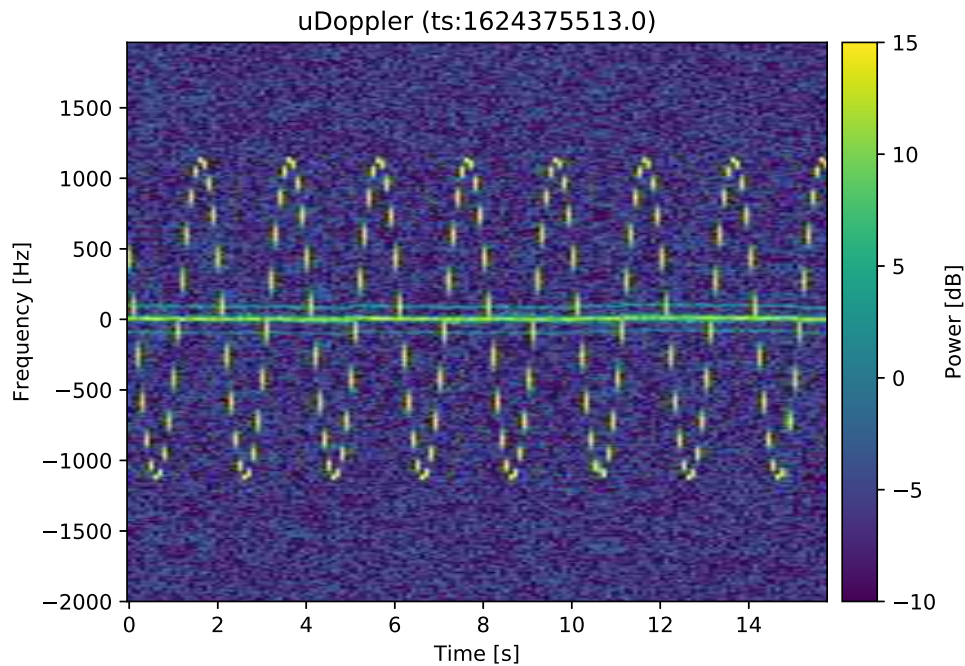


Figure 4.7: Micro-Doppler measurement of a RTS simulation.

### 4.3.2 Windpark simulation set-up

A wind park radar signature simulation experiment was set up on the roof of Palindrome's office building in Landquart, Switzerland. The SAMURAI radar with one transmitter and one receiver node was employed together with two target simulators that were equipped with windpark Doppler and RCS modulation capability. Each target simulator was capable to modulate incoming radar pulses with with Doppler-RCS signatures that correspond to those generated by multiple wind turbines. In addition, each target simulator was also equipped with the capability to generate a second target behind the first target. This second target can also be modulated with wind park Doppler-RCS signatures. With this combination of two target simulators, multiple targets per target simulator and multiple windmills per target, a wealth of different simulation combinations that mimic radar returns of arbitrary windparks can be generated.

### 4.3.3 Wind Park with Two Windmills

The software and the FPGA of the RTS is extended according to the description in Section 2.6, such that the RTS is able to simulate wind farms.

The figures in this section show the micro-Doppler frequencies changing with time at a fixed range bin. The RTS is able to simulate windmills at more than one range bin and this micro-Doppler signature looks similar to the figures shown here.

The first measurement of two windmills is very simple. Both windmills are modeled by one single blade while each blade is modeled with a single scatterer. In Section 3.8.1 the simulation of this setting is discussed. Figure 4.9 shows the corresponding measurement. The rotation speed was set to 15 RPM for the first and 25 RPM for the second windmill, leading to a maximal Doppler frequency of 1460 and 1870 Hz, respectively.

Measurements of two windmills with three blades are shown in Figure 4.10. Each blade is modeled by a single scatterer. The rotation speed was set to 20 RPM (1196 Hz maximal Doppler frequency) for the first and 30 RPM (2243 Hz) for the second windmill.

A realistic measurement of two windmills is shown in Figure 4.11. This experiment is based on the the



Figure 4.8: Set-up of the wind park simulation experiment on the roof of our office building in November 2022. (a) Radar receiver in the foreground, target simulator and transmitter in the background. (b) Image of the radar receiver.

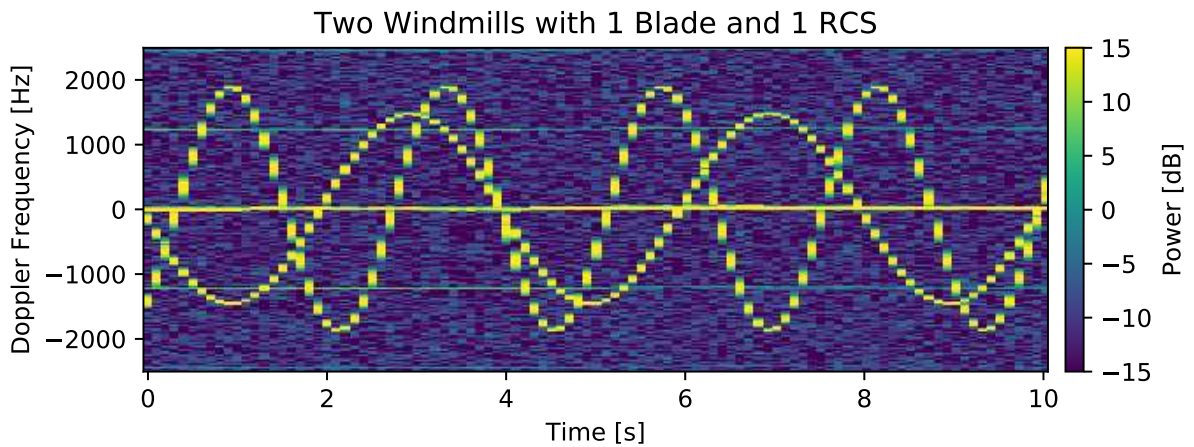


Figure 4.9: Micro-Doppler measurement of a RTS simulation. Two windmills are simulated, both with one single blade while each blade is simulated by a single scatterer. The rotation speed is set to 15 RPM for the first and 25 RPM for the second windmill.

same two windmills that were already shown in Figure 4.9 with the difference that now each windmill is simulated with three blades and each blade is modeled by 10 and 15 scatterers. Furthermore, the RCS of each scatterer has a dependency on the rotational angle of the corresponding blade. This is done to simulate the so-called blade flashes. It needs to be noted that the blade flash is not very pronounced in the shown measurement.

#### 4.3.4 Wind Park with Four Windmills

For the measurement of four windmills, two RTS are used. Each RTS simulated two windmills. The RTS are located relatively close to each other such the the radar is able to see the signatures of all windmills from the same azimuth direction.

The measurement result is shown in Figure 4.12. In this figure only one RTS was simulating two windmills during the first two seconds. At Second Two the second RTS was switched on such that all four windmills could be simulated. The windmills have rotational speeds of 15, 20, 25 and 30 RPM, corresponding to 1460, 1196, 1870 and 2243 Hz of maximal Doppler frequency. The windmill with 30 RPM

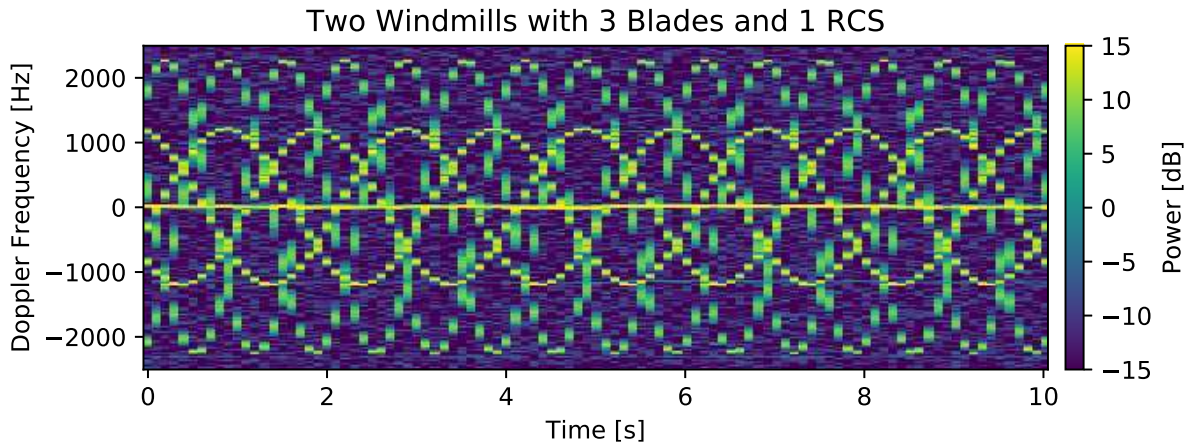


Figure 4.10: Micro-Doppler measurement of a RTS simulation. Two windmills with 3 blades that are modeled with a single scatterer are simulated. The rotation speed is set to 20 RPM for the first and 30 RPM for the second windmill.

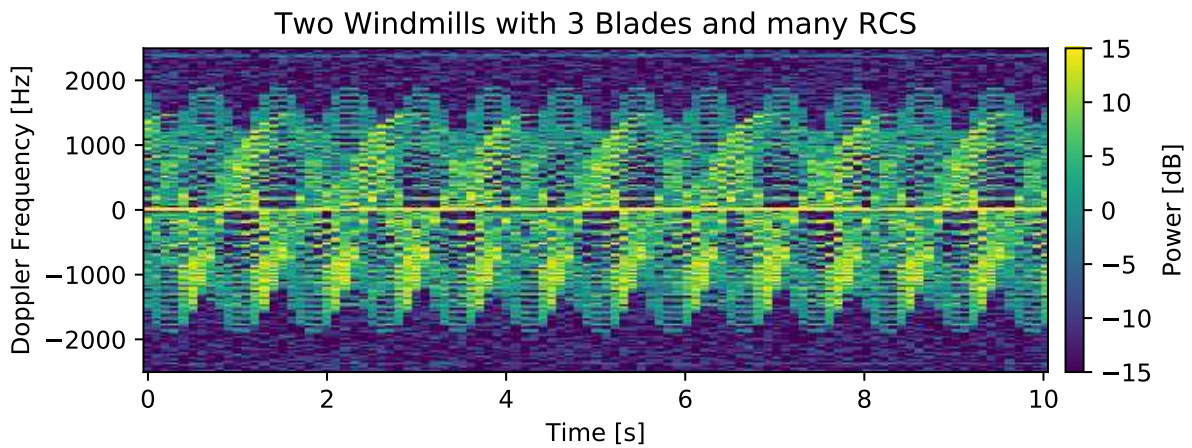


Figure 4.11: Micro-Doppler measurement of a RTS simulation. The same two windmills that are shown in Figure 4.9 are simulated. Three blades are modeled with 10 and 15 scatterers while the scatterer's intensity is modeled with a dependency on the rotational angle.

(2243 Hz) is difficult to see for reasons that have not yet been fully investigated.

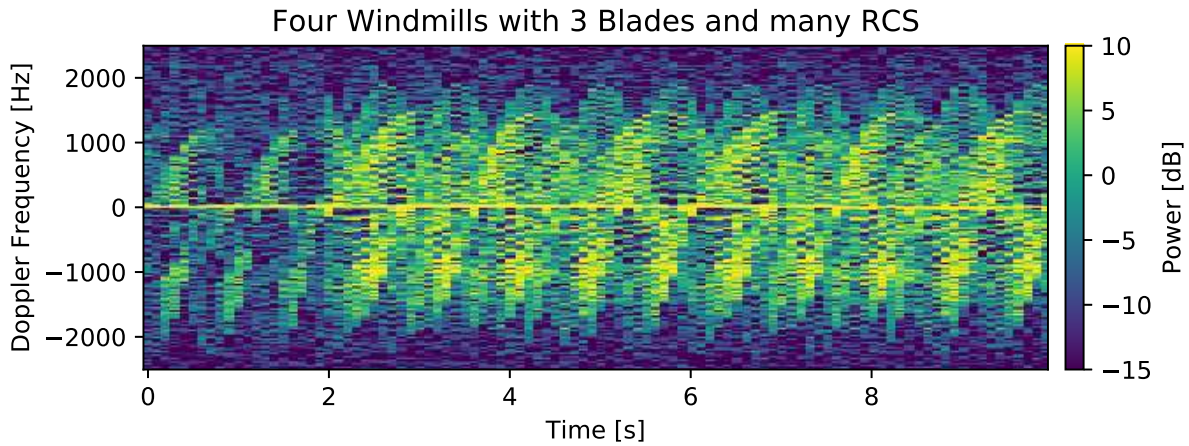


Figure 4.12: Micro-Doppler measurement of four windmills. During the first two seconds, the simulation of two windmills was switched off. Starting from Second 2, four windmills can be seen with 15, 20, 15 and 30 RPM. The windmill with 30 RPM and the highest maximal Doppler frequency appears weak.

## 4.4 Validation

Comparing Fig. 4.10 with Fig. 4.6 and Fig. 4.5 allows to draw conclusions on the validity of the proposed method. Comparisons can be made only qualitatively for the following reasons:

- Fig. 4.5 contains two wind turbines. However, the figure has a limited Doppler resolution and data stems from a different radar than the one that was used for the measurements of the RTS generated RCS-Doppler signatures.
- Fig. 4.6 contains only one wind turbine, while the sophisticated RTS simulations in Fig. 4.10 and Fig. 4.12 contain two and four wind turbines, respectively.

Nevertheless it is seen that the sophisticated RCS-Doppler signatures generated with a target simulator can mimic real wind turbines. Doppler and RCS values can be adjusted in the target simulator such that similarities with real turbines can be optimized. In addition, rotational blade speeds can also be adapted. The simulation of the blade flashes did not lead to features in the radar data as pronounced as seen in Fig. 4.6. However, blade flash effects are clearly visible in Fig. 4.10 and Fig. 4.12.

The received power in the measurements of the generated windmill is approximately 15 dB lower than what has been measured with the real wind turbine in Fig. 4.7 (the power levels measured in Fig. 4.5 are arbitrary digital units and hence cannot be compared). This power level however strongly depends on the distance of the radar to the wind turbine.

Several wind turbines within one radar range gate lead to a rather blurred image with less distinct features, as seen in Fig. 4.5. The simulation in Fig. 4.10 and Fig. 4.12 can well reproduce such blurred signatures. Some details were not included in the simulations for complexity reasons, e.g., the clearly visible shadow that stems from the mast as seen in Fig. 4.7. It is assumed that such details vanish if wind turbines or wind parks are observed from a distance larger than a couple of kilometers, which is usually the case in real-world scenarios where the radar is located in a reasonable distance from any wind turbines.



## Chapter 5

### Outlook

- The windmill simulator delays radar pulses with a constant time offset. More realistic simulations can be achieved by extending the model and allowing radar pulses to be delayed by a discrete number of different time offsets.
- It seems feasible to replay pre-recorded micro-Doppler characteristics of a windmill. To do so, filtering and interpolation procedures need to be applied to the recorded radar measurements.



# Acronyms and Glossary

CPI	coherent processing interval
DFT	discrete fourier transform
FPGA	Field-programmable gate array
PRF	pulse repetition frequency
PRI	pulse repetition interval
RAM	random access memory
RCS	radar cross section
RPM	revolutions per minute
RTS	radar target simulator



# Bibliography

Schneebeli, M., A. Leuenberger, U. Siegenthaler, and P. Wellig, 2020: Testing a multistatic C-band radar with a target simulator. *International Radar Symposium 2020*, IEEE, Warsaw, Poland.